The Astrophysical Journal, 618:1039–1043, 2005 January 10

MODELS FOR SOLAR MAGNETIC LOOPS. V. A NEW DIAGNOSTIC TECHNIQUE TO COMPARE LOOP MODELS AND OBSERVATIONS

E. Landi
Artep, Inc., Ellicott City, MD 21042; and Naval Research Laboratory, Washington, DC 20375-5320

and

M. Landini
Universita' degli Studi di Firenze, Largo E. Fermi 2, 50125, Florence, Italy
Received 2004 August 4; accepted 2004 September 17

ABSTRACT

We present a new diagnostic technique to compare theoretical models with observations of quiescent magnetic loops from high-resolution imaging spectrometers. The diagnostic technique is primarily suited for the analysis of high-resolution, spatially resolved spectra, but it can also be applied to narrowband images. The diagnostic technique is based on a steady state, dynamic loop model and allows us to unambiguously determine whether the model reproduces the observations and to determine the plasma heating, velocities, footpoint conductive flux, and pressure in the loop.

Subject headings: hydrodynamics — plasmas — Sun: magnetic fields

1. INTRODUCTION

Plasma loops are one of the most fundamental components of the solar outer atmosphere and play a major role in the quiet Sun, active regions, and flares as far as the morphology, dynamics, and energetics of those regions are concerned. The ability to accurately measure the physical properties of such structures and to compare them to theoretical models is of maximum importance for the understanding of their origin, their evolution, and the mechanism(s) that heat their plasma.

In the recent past, the wealth of observations of loops in the solar atmosphere provided by the *Yohkoh*, *SOHO*, and *TRACE* satellites has led to a renewed interest in loop physics. For the first time, *Yohkoh*, *SOHO* EIT, and *TRACE* were able to monitor the temporal evolution of solar loops for hours with unprecedented temporal and spatial resolution; the imaging spectrometers on board *SOHO* have provided high-resolution monochromatic images of loops in spectral lines suitable for plasma diagnostics. This wealth of data has triggered a vast number of new studies that attempted to compare theoretical models with loop observations.

Such comparisons have been carried out mostly by measuring the temperature and density profiles using line intensity ratios from spectrometers or filter ratios from narrowband imagers. Measured profiles have been compared with theoretical predictions to validate or dispute the predictions made by the models. In addition, they have provided important information on loop heating: Priest et al. (1998, 2000) demonstrated that temperature profiles are strongly influenced by the assumed shape of the loop heating, so that a successful comparison of measured and observed temperature profiles could in principle be a powerful diagnostic tool for loop heating.

However, the measurement of temperature profiles in loops has been the subject of a heated debate. Measurements have been carried out using filter ratios from narrowband imagers (Neupert et al. 1998; Aschwanden et al. 1999, 2000; Lenz et al. 1999; Priest et al. 1998, 2000), line intensity ratios (Brković et al. 2002; Landi & Landini 2004), and differential emission measure (DEM) analysis (Schmelz et al. 2002; Schmelz 2002; Martens et al. 2002); while all these studies agree that loop temperature profiles are relatively constant along the loop axis, no consensus has been reached on whether the plasma across the loop section is multithermal or not. However, temperature measurements from imagers have been shown to be often ambiguous (Testa et al. 2002; Chae et al. 2002); measurements from line ratios, DEM, and emission measure analysis from spectrometers have provided contradictory results in terms of loop isothermality along the line of sight. In addition, measurements from the existing spectrometers have the additional disadvantage of a limited spatial resolution, so that loop shape selection and background subtraction become crucial issues, especially when the loop shape is divided into smaller subsets to determine the temperature at many positions along the loop. Moreover, if several ratios from different ions are used, the measured temperatures may be different and it is not easy to understand whether those differences are due to real plasma multithermality, blending, or atomic physics problems. In addition, the measurement of electron densities requires line pairs suitable for density diagnostics, not readily available in many wavelength ranges. The measurement of loop filling factors can be done with spectral lines, but it is difficult to do with narrowband images; yet, it is of maximum importance to understand the filamentary structure of loops.

In the present work we have developed a new diagnostic technique that allows the comparison of theoretical loop models and observations by using simultaneously all the spectral lines observed in a loop and dispensing from all other plasma diagnostic techniques and their requirements. This new diagnostic technique is the application to a more sophisticated model of the idea developed by Landini & Landi (2002). This technique allows us to investigate easily the space of parameters of the loop model and to unambiguously determine whether there is agreement or not. This diagnostic technique also allows us to investigate the loop heating function and does not have the ambiguities of the line or narrowband filter ratio techniques, since it considers simultaneously all the fluxes of the observed spectral lines or filters integrated over the whole loop structure. No assumption of plasma isothermality is necessary, and if a line is blended or has atomic physics problems, it can easily be

identified and removed from the data set. In addition, all lines are suitable for this diagnostic technique, regardless of their temperature or density dependence. The use of fluxes integrated over the whole loop structures also increases the signal-to-noise ratio for each spectral line, so that fainter lines can also be used and uncertainties due to background subtraction can be minimized.

The theoretical model that constitutes the basis of the diagnostic technique is introduced in § 2; the diagnostic technique and a few examples are described in § 3, while § 4 discusses the applicability of this technique and summarizes the present work.

2. THEORETICAL MODEL

The loop model the new diagnostic technique is based on is described in Landi & Landini (2004). Here we limit ourselves to recalling its basic features and the equations necessary for the diagnostic technique. The loop model developed by Landi & Landini (2004) consists of a one-dimensional, stationary, nonstatic model in which velocities are nonnegligible and subsonic everywhere in the loop, so that shocks cannot develop at any point. The loop is also assumed to be toroidal, and with constant cross section. The model solves the equations of conservation of mass, momentum, and energy, making use of the equation of state and considering, in the energy equation, radiative losses, energy conduction, dynamic terms, and an unknown heating (H), whose functional shape is selected by the user.

Landi & Landini (2004) introduced scaling laws to simplify the equations and limit the number of free parameters in the model. They defined the scaled temperature, density, velocity, pressure, conductive flux, and position along the loop, t, ρ', x, p, f, and θ, as

$$T = tT_M, \tag{1}$$

$$\rho = \rho' \frac{\sqrt{A}\pi T_M^2}{L}, \tag{2}$$

$$v = x\sqrt{aRT_M}, \tag{3}$$

$$P = p\sqrt{A}R\pi \frac{T_M^3}{L}, \tag{4}$$

$$F_C = f \frac{A\pi T_M^{7/2}}{L}, \tag{5}$$

$$z = \theta \frac{L}{\pi}, \tag{6}$$

where the reference temperature T_M is arbitrarily chosen as 10^6 K (its choice does not have consequences on the model), L is the total length of the loop, measured from observations, $A = 0.92 \times 10^{-6}$ ergs cm^{-1} s^{-1} K$^{-7/2}$, $R = 8.31 \times 10^7$ ergs mol^{-1} K^{-1}, a is the parameter that controls the plasma velocity in the loop, and can be chosen by the user, and T, ρ, v, P, F_C, and z are the true temperature, density, velocity, pressure, conductive flux, and position along the loop.

When we use these scaling laws, the model can be expressed as a function of only three quantities: scaled temperature t, scaled density ρ', and scaled conductive flux f, all functions of the angle θ defined by equation (6), which corresponds to the distance z along the loop. The equations of state, of the conductive flux, and of the conservation of mass, momentum, and energy can be expressed as

$$p' = \frac{t}{x}, \tag{7}$$

$$\frac{dt}{d\theta} = -\frac{f}{t^{5/2}}, \tag{8}$$

$$x\rho' = 1, \tag{9}$$

$$\frac{d\rho'}{d\theta} = \frac{\rho'}{t^{5/2}} \frac{K_0(\theta) t^{5/2} - f}{a - \rho'^2 t}, \tag{10}$$

$$\frac{df}{d\theta} = \frac{G_0 a^{1/2}}{t^{5/2}} \left[t\rho'^2 \frac{K_0(\theta) t^{5/2} - f}{a - \rho'^2 t} + \frac{f}{\gamma + 1} \right] + \frac{L}{\pi A T_M^{7/2}} H(\theta) - C \frac{\rho'^2}{t^{1/2}} \epsilon(t), \tag{11}$$

where

$$K_0(\theta) = \frac{L}{\pi R T_M} \frac{GM_\odot}{\left(R_\odot + R_{\rm loop} \sin\theta\right)^2} \cos\theta \cos\alpha,$$

$$G_0 = \sqrt{\frac{R^3}{A}}, \quad H(\theta) = H_0 h(\theta), \tag{12}$$

where α is the inclination of the loop's plane relative to the normal direction, $C = 2.55 \times 10^{47}$ g^{-2}, $\epsilon(t)$ is the plasma emissivity, $\gamma = 5/3$, $R_\odot$ is the solar radius, H_0 is the amplitude of the heating, and $h(\theta)$ is normalized to 1.

Equations (7)–(11) can be solved using the scaled length θ, and the integration is carried out for $\theta = 0$ to $\theta = \pi$. The numerical integration is performed with a variable space grid, determined by imposing that the difference in temperature and radiated energy between two adjacent grid points be smaller than 10% and 1%, respectively. The temperature of both loop footpoints is arbitrarily chosen to be 10^4 K. The input parameters are

1. the total loop length $L_{\rm loop}$ (from observations),
2. the inclination α of the loop plane relative to the vertical (from observations),
3. the plasma pressure p_0 at the footpoint with $\theta = 0$ (from observations or chosen by the user),
4. the velocity parameter a (chosen by the user),
5. the conductive flux at the footpoints F_0 (chosen by the user),
6. the shape of the energy input $h(\theta)$ (chosen by the user).

$L_{\rm loop}$ and α are determined from narrowband or monochromatic images, and p_0 can be measured from density- and temperature-dependent line ratios in case they are available; otherwise it can be chosen by the user. Once these six parameters are defined, the loop model is completely defined.

The use of $L_{\rm loop}$ and α as input parameters derived from the observations allows to fix the gravity effects, so that the radiative losses and the energy balance depend only on p_0, a, F_0, and $H(z)$. Therefore, once these parameters are selected (or, in the case of p_0, measured) by the user, the amplitude of the heating H_0 is also fixed and can be evaluated by using an iterative procedure that determines the value of H_0 that allows the temperature of the right-hand footpoint ($\theta = \pi$) to be 10^4 K.

3. THE DIAGNOSTIC TECHNIQUE

The flux at distance d of an optically thin line emitted by the *whole* loop is given by

$$F_{\rm obs} = \frac{1}{4\pi d^2} \int G(T) N_e^2 \, dV, \tag{13}$$

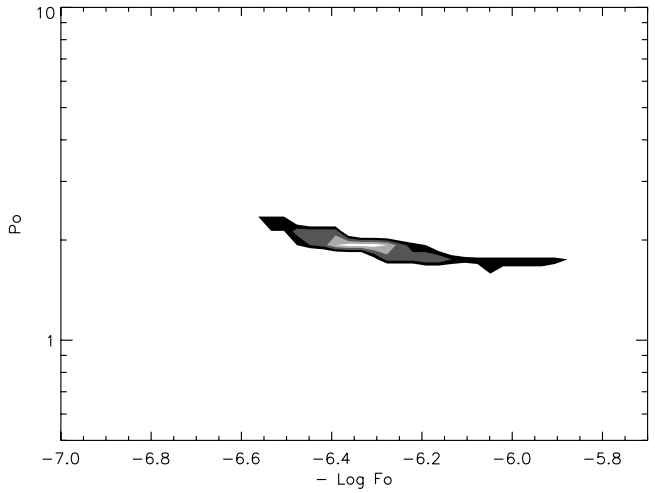

FIG. 1.—Loop diagnostic technique for the simultaneous measurement of p_0 and F_0 for the case in which the velocity parameter a is fixed. The R curves have been calculated using as observed fluxes the predicted fluxes obtained from the theoretical model, adopting $a = 0$, $F_0 = -2.82 \times 10^6$ ergs cm^{-2} s^{-1}, and $p_0 = 1.89$ dyn cm^{-2}. Contour levels indicate the regions in the (F_0, p_0) space where 50%, 64%, 79%, and 93% of the observed lines have a value of 1.0 ± 0.1.

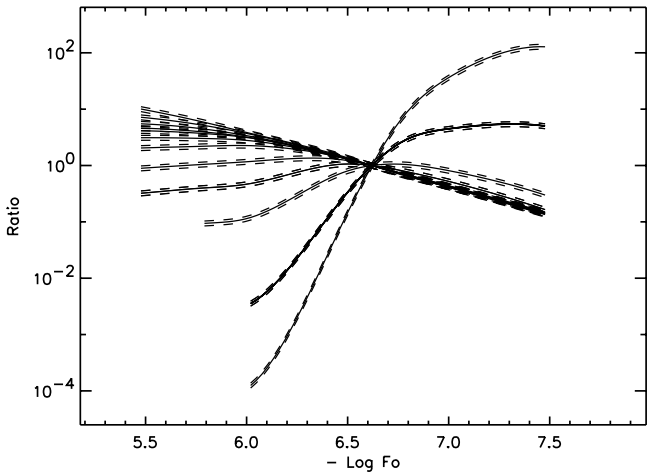

FIG. 2.—Loop diagnostic technique for the measurement of F_0 for the case in which p_0 and the velocity parameter a are known. R curves have been calculated using as observed fluxes the predicted fluxes obtained from the theoretical model, adopting $a = 0$ and $p_0 = 2.5$ dyn cm^{-2}.

where $G(T)$ is the contribution function of the line and the integration is carried out over all the loop volume. By using the theoretical model, the observed flux can be expressed as

$$F_{\rm obs} = -\frac{A_l A T_M^4}{4d^2 b^2 L} \int G(T) \rho'^2 \frac{t^{5/2}}{f}\, dt, \qquad (14)$$

where $b = 1.93 \times 10^{-24}$ g is the proportionality constant between the electron number density N_e and the plasma mass density ρ and A_l is the loop cross section. Similarly to Landini & Landi (2002), we can define the function J as

$$J(H,\ a,\ F_0,\ p_0) = -\int G(T) \rho'^2 \frac{t^{5/2}}{f}\, dt, \qquad (15)$$

and we can also define the ratio

$$R(H,\ a,\ F_0,\ p_0) = \frac{F_{\rm obs}}{J} = \frac{A_l A T_M^4}{4d^2 b^2 L} \frac{J\left(H_*,\ a_*,\ F_{0,*},\ p_{0,*}\right)}{J(H,\ a,\ F_0,\ p_0)}, \qquad (16)$$

where H_*, a_*, $F_{0,*}$, and $p_{0,*}$ are the parameters of the *real* loop. The ratio $R(H, a, F_0, p_0)$ can be defined for all the spectral lines observed in the loop; different lines may have very different R curves in the (H, a, F_0, p_0) space. However, when $(H,\ a,\ F_0,\ p_0) = \left(H_*,\ a_*,\ F_{0,*},\ p_{0,*}\right)$, all the curves will have the same value

$$R\left(H_*,\ a_*,\ F_{0,*},\ p_{0,*}\right) = \frac{A_l A T_M^4}{4d^2 b^2 L}. \qquad (17)$$

The diagnostic technique consists of the calculation of the ratios $R(H, a, F_0, p_0)$ for all the spectral lines observed from a loop in the solar atmosphere. The calculation is carried out after solving the loop model for a chosen H and a grid of a, F_0, and p_0 values. All the curves are then compared together in order to find the common point $R(H_*, a_*, F_{0,*}, p_{0,*})$ where they have the same value. In case the common point exists, the loop model reproduces the observations, a_*, $F_{0,*}$, $p_{0,*}$ can be measured, the adopted heating H is confirmed, and from the value of all the ratios in that point we can also measure the loop cross section A_l; this cross section can be compared to the value measured from line or narrowband intensity maps of the solar loop, so that the filling factor of the loop itself can be evaluated. The filling factor allows us to check whether the loop is monolithic or is composed of subresolution strands. In case p_0 is known from line intensity ratios, the R curves will depend only on H, a, and F_0. If velocities are negligible along the whole loop, a can be assumed to be zero, and the R curves will depend only on F_0 and p_0. The existence of a common crossing point also confirms the choice of the functional form of the heating; if there is no common crossing point, the heating function is incorrect and needs to be changed or its parameters, if any, varied.

The diagnostic technique is implemented in four steps.

1. An analytical function is selected to describe the heating $h(\theta)$.
2. The model is solved for a grid of a, F_0, and p_0 values.
3. The ratios $R(a, F_0, p_0)$ are calculated for all the lines.
4. The region in the (a, F_0, p_0) space is explored to find the point where all the curves have the same value.

An example of this technique is given in Figure 1 for the case where a is fixed. In Figure 1, the (F_0, p_0) space is divided in a grid of intervals and the number of R curves that pass through each element of the grid is counted; the contours indicate the areas where 50%, 64%, 79%, and 93% of the lines are found. The R curves have been calculated by using, as observed fluxes, the fluxes calculated adopting $a = 0$, and $F_0 = -2.82 \times 10^6$ ergs cm^{-2} s^{-1}, and $p_0 = 1.89$ dyn cm^{-2}: in this case, the R curves will be equal to unity in their common crossing point. The heating has been assumed to be uniform. To check the effect of experimental uncertainties on the diagnostic technique, we have assigned to each simulated flux an artificial 10% uncertainty. Figure 1 shows that for that set of F_0 and p_0 values, a rather precise diagnostics of both F_0 and p_0 is possible. The artificial uncertainty causes the region where 93% of the lines cross to be wider than the grid size.

In the case where velocities are negligible, the R curves depend only on H, F_0, and p_0, and once H is selected the diagnostic technique can be simplified to two parameters only: F_0 and p_0. If also p_0 is known, once the heating H is selected

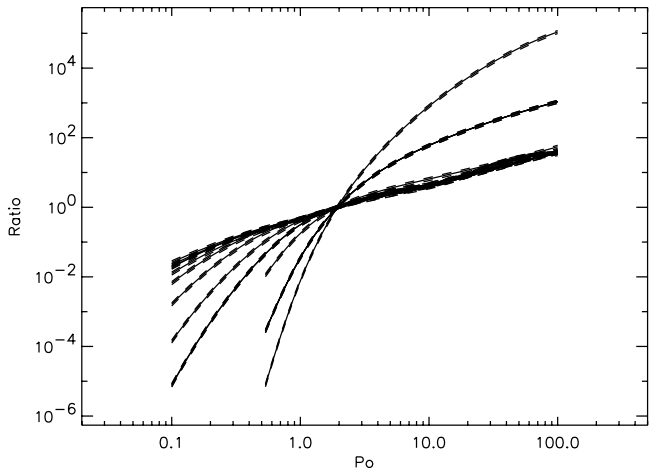

FIG. 3.—Loop diagnostic technique for the measurement of p_0, when F_0 is known and velocities, characterized by the parameter a, are low enough not to be measurable with the diagnostic technique. R curves have been calculated using as observed fluxes the predicted fluxes obtained from the theoretical model, adopting $a = 0$ and $F_0 = 3.16 \times 10^5$ ergs cm^{-2} s^{-1}.

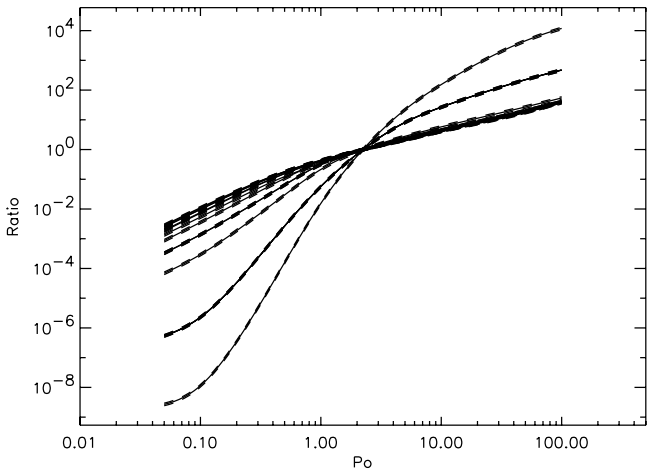

FIG. 5.—Same as Fig. 3, in the case with exponential heating concentrated at the loop top. R curves have been calculated using as observed fluxes the predicted fluxes obtained from the theoretical model, adopting $a = 0$ and $F_0 = -7.94 \times 10^5$ ergs cm^{-2} s^{-1}.

and the R curves calculated, it is possible to display all the R curves in the same figure as a function of F_0 alone: in case the model is able to reproduce the observations, all the curves R will meet in the same crossing point. An example is given in Figure 2, where R curves have been calculated using as observed values the predicted fluxes obtained with $a = 0$, $p_0 = 2.5$ dyn cm^{-2}, and uniform heating. The R curves are calculated as a function of F_0 only and reported in Figure 2, which shows that F_0 can be measured with accuracy. The uncertainty arbitrarily associated to each R curve is 10%. A similar example, obtained by fixing a and p_0, is given in Figure 3, where the R curves obtained by choosing $a = 0$, $F_0 = 3.16 \times 10^5$ ergs cm^{-2} s^{-1}, and uniform heating are displayed as a function of p_0, to show that a very accurate loop diagnostic and measurement of p_0 are also possible. Similar examples are displayed in Figures 4 and 5, where the diagnostic technique, in the cases where both a and F_0 or p_0 are fixed, is applied to the case in which the input is exponential, concentrated at the top, with a scale height of 10,000 km. As in the uniform heating case, the diagnostic technique allows a very precise determination of F_0 and p_0, as well as a determination of whether the loop model reproduces the observations.

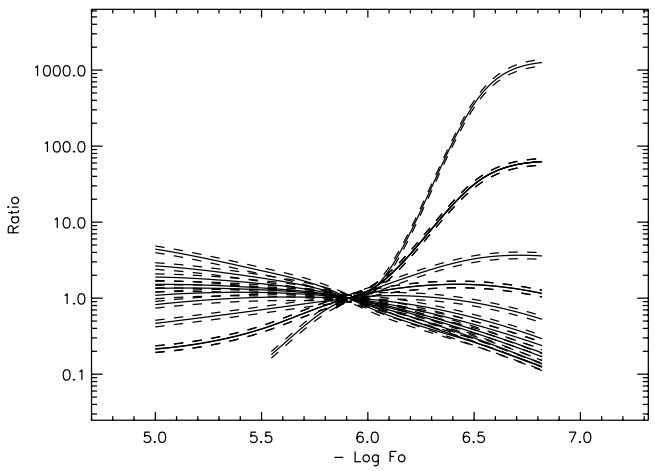

FIG. 4.—Same as Fig. 2, in the case with exponential heating concentrated at the loop top. R curves have been calculated using as observed fluxes the predicted fluxes obtained from the theoretical model, adopting $a = 0$ and $p_0 = 1.99$ dyn cm^{-2}.

4. DISCUSSION AND CONCLUSIONS

The present diagnostic technique is a very powerful tool for comparing loop models and observations. One of its most important characteristics is that it requires only a handful of spectral lines to be carried out, and it is not necessary that such lines are density sensitive relative to each other. This feature allows us to carry out detailed comparisons between loop model and observations also in the cases where only a few lines are available or no plasma diagnostic is possible using the standard techniques. For example, this technique makes it possible to analyze in detail many available loop observations obtained with the SUMER instrument on board *SOHO*: these very high spatial and spectral resolution data sets are limited by the paucity of lines transmitted to the ground and cannot be investigated with traditional diagnostic techniques in most cases. The present diagnostic technique is also well suited for the analysis of data sets from future NASA missions such as EUNIS, *Solar-B*, *STEREO*, and *SDO*.

However, there are a few points that need to be discussed. Figures 2 through 5 show that lines formed at similar temperatures provide curves that depend on F_0 and p_0 in a very similar way; the same can be said for the case when the diagnostic is carried out using all three parameters a, F_0, and p_0. This means that it is necessary to include in the set of lines to be analyzed lines emitted at very different temperatures: chromosphere, transition region and corona. In fact, the greatest sensitivity to changes of the parameters a, F_0, and p_0 is found in lines emitted by ions whose temperature of maximum abundance is close to the range of loop maximum temperatures in the grid. In fact, changing the loop parameters has two main effects on the loop: the top temperature changes (usually, the higher the parameter values, the higher the top temperature), and the DEM of the loop increases. However, the DEM curves of models obtained with a different choice of parameters have a similar shapes, so that all the predicted line intensities will change in a very similar way. Figure 6 shows the DEM curves of the loop model as calculated using a grid of F_0 and p_0 parameters: all the curves are approximately parallel, and the main difference is due to the higher or lower loop top temperature. The only lines whose R

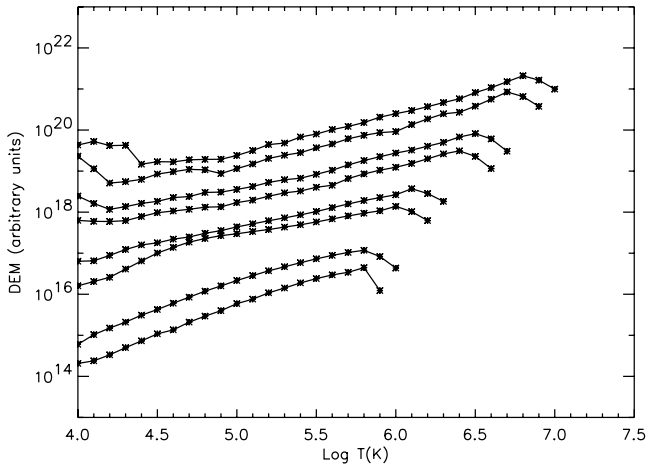

FIG. 6.—DEM curves calculated by the loop model adopting a grid of values for F_0 and p_0.

functions will exhibit a different behavior as a function of the loop parameters will be those whose temperature of maximum abundance is close to the range of loop top temperatures, because in their cases significant amounts of plasmas at temperatures higher than those reached by other models contribute to the total intensity of the loop.

If a spectral line is blended or is affected by atomic physics problems, it can be easily identified and discarded from the analysis, since it will behave differently from all the other lines from the same ion or from ions formed at very similar temperatures. In addition, Landi & Feldman (2004) have shown that the loop footpoints, where the bulk of the chromospheric and transition region emission of the loop is concentrated, are very faint and it is difficult to distinguish them from the background. Therefore, in order to measure cold lines and be able to obtain accurate results from the present diagnostic technique, it is necessary to use spectra obtained with high spatial resolution instruments. The future spectrometers and narrowband imagers will be equipped with telescopes and detectors with sufficient spatial resolution and spectral coverage to allow the use of the present diagnostic technique.

Background subtraction is of crucial importance for reliable loop diagnostics, especially in the case of limited spatial resolution (i.e., Brković et al. 2002; Schmelz et al. 2003). Background subtraction is even more important when the loop shape is divided into many different segments to measure the physical properties along the loop axis with traditional diagnostic techniques, since intensities in each segment may be rather low and therefore background-subtracted intensities may have very large uncertainties. One advantage of the present diagnostic technique is that it requires that intensities be summed over the whole loop shape, so that line intensities are higher and uncertainties in the background-subtracted intensities lower.

In principle, the present diagnostic technique can be used with narrowband imagers, thus enabling us to study data sets with the highest spatial resolution and best loop observations available. The only difference is that it is necessary to include the filter-weighted emissivity in the calculation of the observed flux instead of single-line emissivities. A possible problem with imagers is, however, that they mostly use coronal lines, so the accuracy of the diagnostics might be limited in the case in which the loop observed top temperature is far from the temperature of maximum response of the imagers' filters.

The present diagnostic technique can also be used with models with variable cross section: for them it is necessary to calculate the R curves also as a function of the parameters of the cross section itself. The diagnostic technique can still be applied in these cases, although the R curves are dependent on the variable cross section parameters. The basic equations (eqs. [16] and [17]) are still valid and the four steps of the diagnostic technique can still be implemented, provided the R curves are calculated for a grid of values that includes also the new parameters: then, determining whether a common point to all the curves exists or not is relatively straightforward.

The lack of a common crossing point has important diagnostic consequences, as it indicates that the heating function adopted to solve the equations and calculate the R functions is incorrect. This means that either the parameters of the heating need to be varied, or that the functional form $h(\theta)$ of the heating needs to be changed.

We plan to apply the present diagnostic technique to existing SUMER observations of active region loops where no lines are available for direct density and temperature diagnostics, but several lines formed at very different temperatures are observed, in an effort to understand the heating of loop plasma. This work will be the topic of a separate publication.

The work of E. L. was supported under the NNH04AA12I and W10,232 NASA grants. We thank the referee for his/her comments that helped improving the original manuscript.

REFERENCES

Aschwanden, M. J., Alexander, D., Hurlburt, N., Newmark, J. S., Neupert, W. M., Klimchuk, J. A., & Gary, G. A. 2000, ApJ, 531, 1129
Aschwanden, M. J., Newmark, J. S., Delaboudinière, J.-P., Neupert, W. M., Klimchuk, J. A., Gary, G. A., Portier-Fozzani, F., & Zucker, A. 1999, ApJ, 515, 842
Brković, A., Landi, E., Landini, M., Rüedi, I., & Solanki, S. 2002, A&A, 383, 661
Chae, J., Park, Y. D., Moon, Y.-J., Wang, H., & Yun, H. S. 2002, ApJ, 567, L159
Landi, E., & Feldman, U. 2004, ApJ, 611, L537
Landi, E., & Landini, M. 2004, ApJ, 608, 1133
Landini, M., & Landi, E. 2002, A&A, 383, 653
Lenz, D. D., DeLuca, E. E., Golub, L., Rosner, R., & Bookbinder, J. A. 1999, ApJ, 517, L155
Martens, P. C. H., Cirtain, J. W., & Schmelz, J. T. 2002, ApJ, 577, L115
Neupert, W. N., et al. 1998, Solar Physics, 183, 305
Priest, E. R., Foley, C., Heyvaerts, J., Arber, T. D., Culhane, J. L., & Acton, L. W. 1998, Nature, 393, 545
Priest, E. R., Foley, C., Heyvaerts, J., Arber, T. D., Mackay, D., Culhane, J. L., & Acton, L. W. 2000, ApJ, 539, 1002
Schmelz, J. T. 2002, ApJ, 578, L161
Schmelz, J. T., Beene, J. E., Nasraoui, K., Blevins, H. T., Martens, P. C. H., & Cirtain, J. W. 2003, ApJ, 599, 604
Schmelz, J. T., Scopes, R. T., & Cirtain, J. W. 2002, Adv. Space Res., 30, 507
Testa, P., Peres, G., Reale, F., & Orlando, S. 2002, ApJ, 580, 1159